UAV-based Technique for the Characterization of the Intrinsic Cross-Polarization Ratio (IXR)

Giuseppe Virone [1], Fabio Paonessa[1], Oscar Antonio Peverini[1], Giuseppe Addamo[1], Pietro Bolli[2], Eloy de Lera Acedo[3]
[1] Istituto di Elettronica e di Ingegneria dell'Informazione e delle Telecomunicazioni (IEIIT), Consiglio Nazionale delle Ricerche (CNR), Torino, Italy, giuseppe.virone@ieiit.cnr.it
[2] Osservatorio Astrofisico di Arcetri (OAA), Istituto Nazionale di Astrofisica (INAF), Firenze, Italy
[3] Cavendish Laboratory, Department of Physics, University of Cambridge, Cambridge CB3 0HE, UK

***Abstract*—This paper presents a measurement strategy for the Intrinsic Cross Polarization Ratio (IXR) of Jones polarimeters operating at VHF /UHF bands. It is based on a suitable representation of the Jones matrix which identifies the relevant antenna parameters for IXR evaluation. The same representation is used within a best-fit procedure with experimental results that can be obtained using a rotating UAV-mounted test source.**

***Index Terms*— antenna measurement, polarization measurement, Unamanned Aerial Vehicle, polarimeter calibration, Intrinsic Cross Polarization Ratio, IXR**

I. INTRODUCTION

The Intrinsic Cross-Polarization Ratio (IXR) is a very important figure-of-merit for radio-frequency polarimeters [1]. Such a parameter quantifies the orthogonality of the two channel transfer functions regardless of the adopted reference system. It has been demonstrated that the channel orthogonality directly affects the residual polarimeter error after calibration.

The IXR parameter has already been adopted for the performance evaluation of polarimetric phased arrays for radio astronomy in [2]-[6]. It can be determined from the two complex radiation patterns of the dual-polarized polarimeter antenna system. From the experimental point-of-view, this task is very challenging for low-frequency instruments (VHF, UHF) such as the Square-Kilometer-Array Low-Frequency Aperture Array [7], as well as its pathfinders and precursors. In this framework, the Unmanned Aerial Vehicle (UAV) technology has already been adopted in order to characterize the single-element, embedded-element and array radiation pattern of several antenna configurations [8]-[11]. Fig. 1 shows a dipole antenna fed by an RF source, which has been mounted on a micro UAV in order to operate as a flying test source.

In this paper, the exploitation of a UAV-based test source to characterize the IXR parameters without a complete knowledge of the phase patterns is discussed. The experimental results on both reference antennas and array prototypes will be presented at the conference.

Fig. 1. A micro-UAV equipped with a RF generator and a dipole antenna.

II. PARAMETRIZATION OF THE JONES MATRIX

The IXR formulation has already been developed in [1], for both Jones and Müeller polarimeters. As far as the Jones scheme is concerned, a generic polarimeter response can be described with its Jones matrix

$$\begin{bmatrix} v_a \\ v_b \end{bmatrix} = \begin{bmatrix} J_{a\hat{\vartheta}} & J_{a\hat{\varphi}} \\ J_{b\hat{\vartheta}} & J_{b\hat{\varphi}} \end{bmatrix} \begin{bmatrix} E_{\hat{\vartheta}}{}^{inc} \\ E_{\hat{\varphi}}{}^{inc} \end{bmatrix}, \qquad (1)$$

where v_a and v_b are the voltage output of the two polarimeter channels and $E_{\hat{\vartheta}}{}^{inc}$ and $E_{\hat{\varphi}}{}^{inc}$ represents the two-field components of an incoming plane-wave. It should be noted that the all the terms in (1) depends on the observation angle (ϑ, φ), which is understood for the sake of brevity. In this formulation, the IXR parameter can be directly evaluated as

$$IXR = \left(\frac{\kappa(J)+1}{\kappa(J)-1}\right)^2, \qquad (2)$$

where $\kappa(J)$ is the condition number of the Jones matrix. Moreover, it can be shown (by reciprocity) that the Jones matrix can be directly computed from the radiation pattern of the two polarimeter antennas a and b

$$J \propto \begin{bmatrix} E_{\hat{\vartheta}}{}^{a} & E_{\hat{\varphi}}{}^{a} \\ E_{\hat{\vartheta}}{}^{b} & E_{\hat{\varphi}}{}^{b} \end{bmatrix} \quad (3)$$

where $E_{\hat{\vartheta}}{}^{a}$, $E_{\hat{\varphi}}{}^{a}$ and $E_{\hat{\vartheta}}{}^{b}$, $E_{\hat{\varphi}}{}^{b}$ are the corresponding field components. For example, it should be remembered that a basic antenna configuration for Jones polarimeters consists of a pair of crossed dipoles.

A suitable representation of the Jones matrix has been developed in order to both provide some additional physical insight and to identify which pattern parameter will affect the IXR

$$J \propto \begin{bmatrix} 1 & 0 \\ 0 & e^{j\varphi_{ab}} \end{bmatrix} \begin{bmatrix} 1 & 0 \\ 0 & m_{ab} \end{bmatrix} \begin{bmatrix} cos(\delta_a) & sin(\delta_a)e^{j\varphi_a} \\ -sin(\delta_b)e^{j\varphi_b} & cos(\delta_b) \end{bmatrix} \quad (4)$$

The magnitude and phase of the complex ratio between the radiation pattern of the two polarizations a and b are described with m_{ab} and φ_{ab}, respectively. The two polarization vectors i.e. normalized field components are instead parametrized using the angles δ_a, φ_a, δ_b and φ_b. As shown in Fig. 2, such a parametrization is complete since it can describe all the possible polarization states (only channel a is shown). It should be noted (Fig. 2) that δ coincide with the tilt angle of the polarization ellipse only when φ is equal to zero.

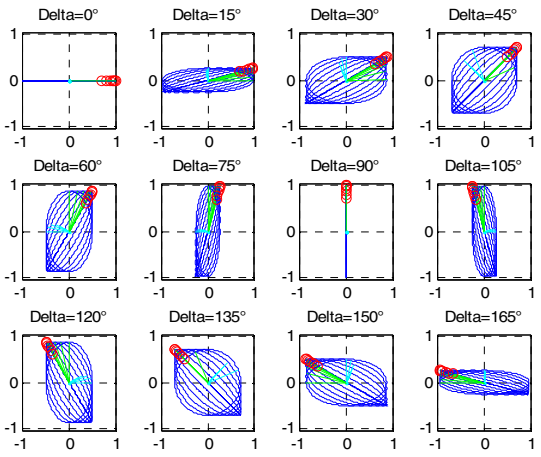

Fig. 2. Polarization ellipses obtained from the parametrization in (4), only channel a is shown. The phase paramter φ_a is swept from -90° to 90° in each plot.

It should be observed that the first matrix in (4) is unitary. Hence, it does not affect the condition number. Therefore, it becomes apparent that the knowledge phase term φ_{ab} is not required to evaluate the IXR. The only required parameters are the relative magnitude m_{ab} and the four angles defining the polarization state of the two channels. Their experimental evaluation is discussed in the next section.

III. UAV-BASED POLARIZATION MEASUREMENT

A suitable UAV-based polarization measurement scheme is shown in Fig. 3. The UAV is programmed to perform a sequence of complete rotations along its vertical axis (variation of the bearing/yaw angle α) at different zenith angles ϑ.

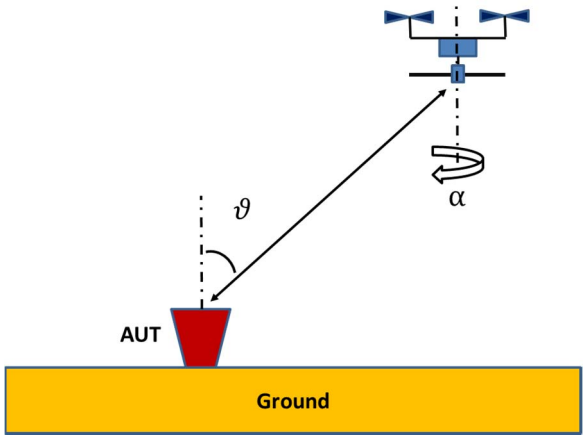

Fig. 3. Scheme of a spin flight above a ground-based Antenna Under Test: α is the UAV bearing (yaw) angle.

At zenith, the incident field to the polarimeter antenna system can be described as

$$E_{\hat{\vartheta}}{}^{inc} \propto cos(\alpha)$$
$$E_{\hat{\varphi}}{}^{inc} \propto sin(\alpha) \quad (5)$$

The polarimeter response can be computed multiplying the column vector in (5) and the parametrized Jones matrix in (4). Only one polarization is discussed hereinafter for the sake of brevity. The amplitude results $|v_a|$ as a function of the bearing angle α, for different values of the parameter δ, are shown in Fig. 4. The effect of the parameter φ for δ=45° is instead shown in Fig. 5.

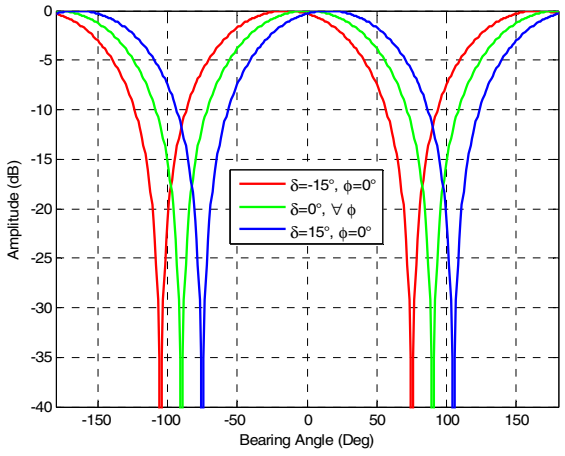

Fig. 4. Amplitude response for a complete spin-flight at zenith (ϑ=0°) for three values of the parameter δ.

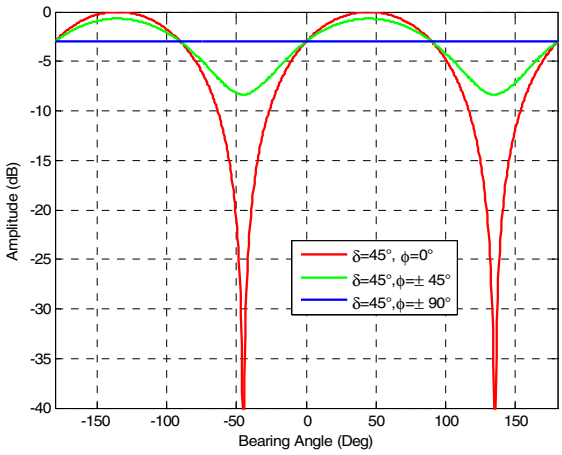

Fig. 5. Amplitude response for a complete spin-flight at zenith (ϑ=0°) for three values of the parameter φ.

It should be noted that only linear polarization cases are shown in Fig. 4, whereas the transition from linear $\varphi = 0°$ to circular $\varphi = 90°$ is shown in Fig. 5 (δ=45°). From both Fig. 4 and 5, it is clear that δ and φ affect the amplitude curve versus bearing angle in a different way. The parameter δ mainly sets the angular position of maxima and minima, whereas φ changes curve dynamics. Examples of experimental results confirming the simulated behaviors can be found in [9]. From the experimental point of view, it becomes apparent that both parameters δ and φ can be evaluated by means of a best-fitting procedure between measured data and the parametrized curves presented above. In particular, the same procedure can be simultaneously applied to both polarimeter polarizations in order to obtain δ_a, φ_a, δ_b and φ_b. The signs of φ_a and φ_b, which determines the right- or left-handedness of the polarization cannot be determined from amplitude measurements. However, it can be shown that both signs can be estimated observing the variation of the phase difference between the two polarizations $\lfloor v_a - \lfloor v_b$ as a function of the bearing angle α (absolute value φ_{ab} in not required). Such phase variation can be evaluated from the cross-correlation product $\langle v_a {v_b}^* \rangle$.
Finally, the parameter m_{ab} in (4) can be evaluated from the ratio between the maximum values of received power (versus bearing angle) for the two channels. Therefore, it can be concluded that all the relevant parameters for the IXR measurement can be evaluated with the proposed technique.

With reference to Fig. 3, it should be noted that the UAV rotation axis is nominally parallel to the ground. Therefore, at observation angles ϑ>0°, the incident field to the polarimeter antenna system during the UAV rotation is also affected by the source pattern, which is not rotationally-symmetric [12]

$$E_{\hat{\vartheta}}{}^{inc} = E^{s}_{\hat{\vartheta}}(\alpha)$$

$$E_{\hat{\varphi}}{}^{inc} = E^{s}_{\hat{\varphi}}(\alpha) \qquad (6)$$

In other words, the relationship between the amplitude response versus bearing angle α and the two parameters δ and φ is not constant with respect to the observation angle ϑ. For example, Fig 6 show the amplitude response for two orientations of the polarimeter antenna δ=0° and δ=90° at an observation angle ϑ=45°. The amplitude difference between the two maxima in Fig. 6 is entirely related to the difference between the test-source E- and H-plane radiation patterns.
As far as the variation of φ is concerned (Fig. 7), the absence of UAV rotational symmetry produce an oscillating curve (blue) even if the polarization is circular for $\varphi = 90°$. Moreover, for δ=45° and $\varphi = 0°$ (red curve) i.e. linear polarization with a tilt angle of 45°, the position of the maximum is actually about 30° instead of 45°.

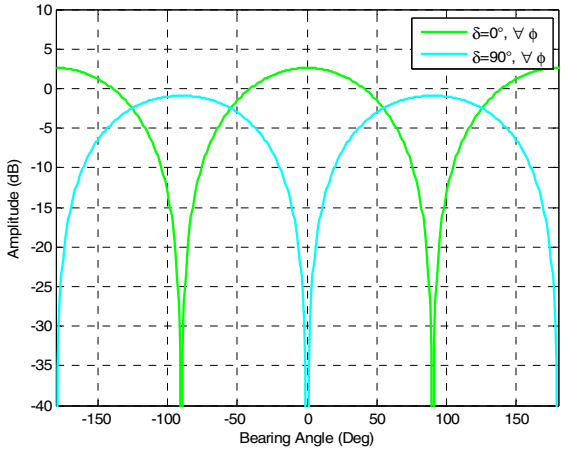

Fig. 6. Amplitude response for a complete spin-flight at zenith (ϑ=45°) for two values of the parameter δ.

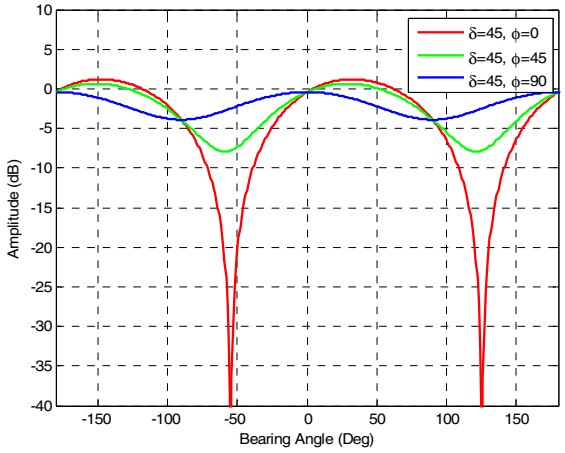

Fig. 7. Amplitude response for a complete spin-flight at zenith (ϑ=45°) for two values of the parameter φ.

The more complex behavior shown in Figs. 6 and 7, requires that the curve parametrization with respect to δ and φ should also include the test source radiation pattern. This task can be accomplished combining (6) and (4).

IV. Conclusion

A measurement method to study the IXR of ground-based low-frequency polarimeters as well as the other polarization characteristics has been proposed. It is based on a sequence of spin flights (rotations of the UAV along its vertical axis) performed at different observation angles. It has been shown that the relevant data can be obtained by means of a best-fitting procedure between measurement data and a set of parametrized curves. The application of such a procedure to real experimental data will be presented at the conference.

References

[1] T. D. Carozzi and G. Woan, "A Fundamental Figure of Merit for Radio Polarimeters", IEEE Trans. Antennas Propag., vol. 59, no. 6, pp.2058-2065, June 2011.

[2] S. J. Wijnholds, "Polarimetry With Phased Array Antennas: Sensitivity and Polarimetric Performance Using Unpolarized Sources for Calibration", IEEE Trans. Antennas Propag., vol. 60, no. 10, pp.4688-4698, October 2012.

[3] B. Fiorelli, M. Arts, G. Virone, E. de Lera Acedo, W. A. Cappellen, "Polarization Analysis and Evaluation for Radio Astronomy Aperture Array Antennas", 7th European Conf. on Antennas and Prop. (EuCAP 2013), Gothenburg, Sweden, 8-12 April 2013.

[4] B. Fiorelli, E. de Lera Acedo, M. Arts, G. Virone, J. G. bij de Vaate, "Polarization performances and antenna misalignment errors for aperture arrays: SKA-low AAVS0.5 case", International Conference on Electromagnetics in Advanced Applications (ICEAA), September 9-13, 2013, Turin, Italy

[5] B. Fiorelli, E. de Lera Acedo, "On the Simulation and Validation of the Intrinsic Cross-Polarization Ratio for Antenna Arrays Devoted to Low Frequency Radio Astronomy", 8th European Conf. on Antennas and Prop. (EuCAP 2014), The Hague, The Netherlands, 6-11 April 2014

[6] A. T. Sutinjo; P. J. Hall, "Intrinsic Cross-Polarization Ratio of Dual-Linearly Polarized Antennas for Low-Frequency Radio Astronomy", IEEE Trans. Antennas Propag., vol. 61, no. 5, pp.2852-2856, May 2013.

[7] J. G. Bij de Vaate ; P. Benthem and H. Schnetler, "The SKA low frequency aperture array ", Proc. SPIE 9908, Ground-based and Airborne Instrumentation for Astronomy VI, 99083X (August 9, 2016); doi:10.1117/12.2231618; http://dx.doi.org/10.1117/12.2231618

[8] G. Virone, et al., "Antenna Pattern Verification System Based on a Micro Unmanned Aerial Vehicle (UAV)," IEEE Antennas and Wireless Propagation Letters, vol.13, pp. 169-172, Jan. 2014.

[9] P. Bolli, et al., "Antenna pattern characterization of the low-frequency receptor of LOFAR by means of an UAV-mounted artificial test source," in SPIE Ground-based and Airborne Telescopes VI, Edinburgh, Scotland, United Kingdom, June 26 – July 1 2016.

[10] P. Bolli, et al., "From MAD to SAD: the Italian experience for the Low Frequency Aperture Array of SKA1-LOW", Radio Science, vol. 51, issue 3, pp. 160–175, Mar. 2016.

[11] G. Pupillo, et al., "Medicina Array Demonstrator: calibration and radiation pattern characterization using a UAV-mounted radio-frequency source," Experimental Astronomy, vol. 39, issue 2, pp. 405-421, June 2015.

[12] G. Virone, et al., "Antenna Pattern Measurement with UAVs: Modeling of the Test Source," European Conference on Antennas and Propagation (EuCAP), Davos, Switzerland, Apr. 11-15 2016.